# ON LINE MEASUREMENT OF CAVITATION EROSION RATE ON A 2D NACA PROFILE

**R. Simoneau**
Hydro-Quebec, Groupe Technologie
Affaires Internationales et IREQ
Quebec, Canada

**F. Avellan and Y. Kuhn de Chizelle**
IMHEF-Institut de Machines Hydrauliques et de Mecanique des Fluides
EPFL-Swiss Federal Institute of Technology of Lausanne
Lausanne, Switzerland

## ABSTRACT

The electrochemical cavitation detection technique has been used to locate and measure the instantaneous cavitation erosion rate on a 2D NACA profile tested in the IMHEF high-speed cavitation tunnel. Nineteen titanium probes, flush mounted along the profile suction side could monitor during the test the local and instantaneous erosion rate with a detection limit as low as 0.02 mm per year of titanium grade 2. Pressure measurements have been also made as well as high speed photography. The operating conditions has been varied in a wide range of velocity, flow incidence and cavitation number. Maximum erosion rate is located in the closure region of the main cavity and is at its highest level for highest cavitation number values compatible with the onset of a leading edge fluctuating cavity. Erosion was associated with the collapse of large transient swirling cavities. These experiments can help to elucidate the basic mechanism responsible for the high cavitation erosion rates observed in large hydraulic machines.

## NOMENCLATURE

| | | | |
|---|---|---|---|
| $L$ | = | Chord length | [m] |
| $p$ | = | Static pressure | [Pa] |
| $p_v$ | = | Vapor pressure | [Pa] |
| $p_0$ | = | Upstream static pressure | [Pa] |
| $U_{ext}$ | = | Outer velocity | [m·s$^{-1}$] |
| $V$ | = | Upstream velocity | [m·s$^{-1}$] |
| $\delta$ | = | displacement thickness | [s] |
| $\rho$ | = | Water density | [kg·m$^{-3}$] |
| $C_p$ | $= \frac{p - p_0}{\frac{1}{2}\rho V^2}$ | Pressure coefficient | [-] |
| $\sigma$ | $= \frac{p_0 - p_v}{\frac{1}{2}\rho V^2}$ | Cavitation number | [-] |
| $\omega$ | = | Cavitation vortex vorticity | [rad·s$^{-1}$] |

## INTRODUCTION

As far as hydro-power is concerned cavitation erosion remains a costly problem in large hydraulic turbines and pump-turbines. Even the best materials, special stainless steels or cobalt base alloys, are eroded at rates reaching many millimeters per year [1-3]. These erosion damages require repair downtimes at regular intervals and cause production losses. Many solutions are available: restricted operation, tougher materials, better conception. The best solution is obviously to optimize [4] the design of the blade leading edge by using for instance an inverse method [5] in order to overcome this problem. Unfortunately it may be much more difficult to achieve for a wide range of operating conditions and even impossible or too costly for existing machines.

The prediction of cavitation erosion at the conception stage is still more an art than a science [6], and metal erosion loss warranty actually given by the designers-manufacturers of large hydraulic turbines is still mainly based on their previous experience with similar designs. Modern computer calculations can predict the location and intensity of low pressure regions that can generate cavitation. But no one can yet predict the erosion rate for a given material that can be produced by this cavitation. It is a complex problem with the interaction between dynamic properties of both flow and materials [7].

Reduced scale model tests provide cavitation data such as the critical cavitation efficiency-cavitation number curves, cavity size and location, and some erosion data by using acoustic, paint, or pressure sensitive coating detection techniques. All these data yield qualitative indications. Complemented with empirical laws based on cumulated experience on prototypes, they are used to establish the required setting level and the safe operating range to avoid unacceptable erosion. These empirical laws cannot be generalized easily and have yielded notable mistakes [8].

More recently a quantitative electrochemical cavitation detector has been used in model turbine tests [9]. These tests have shown in particular that the cavitation erosion rates produced in the model test as they can be done in the existing facilities are much lower than those observed on prototypes even at the same head. These results point out the leading role of the local flow velocity in cavitation erosion, in such a drastic way, that it is possible for the cavitation clouds or vortices causing the erosion on prototype not even to be present in model tests.

To overcome this difficulty of carrying erosion measurements in model tests and in an attempt to eventually establish more accurate erosion scaling laws, Avellan and Dupont [10] have proposed to simulate cavitation erosion of hydraulic turbines on a 2D-NACA profile. They have shown that the severe erosion of turbine runners can be attributed to the development of the fixed cavities attached at the leading edge of the blades [11]. The results reported here are a continuation of this work. The electrochemical cavitation detection technique has been used to locate and measure quantitatively the instantaneous cavitation erosion rate for different flow incidences, velocities and cavitation number values. By addition, pressure measurements and flow visualization are carried out in order to compare the erosion with the leading edge cavity development.

## THE ELECTROCHEMICAL DETECTION TECHNIQUE

Cavitation erosion rates depend on both the cavitation intensity and the resistance of the exposed material. The characterization of cavitation intensity with respect to material erosion is difficult. Some rational attempts, [12], have been made using the acoustic power density radiated from the cavitation collapse. This approach is not very practical since it is difficult to measure and calibrate this power density and also to relate it to erosion. Although cavitation intensity is an intrinsic property of a given liquid flow it can be characterized by the erosion rate of a known material. In this way the erosion of the same known material can be used to compare the erosive power of different flow conditions and also to predict the erosion of other materials, knowing their relative resistance.

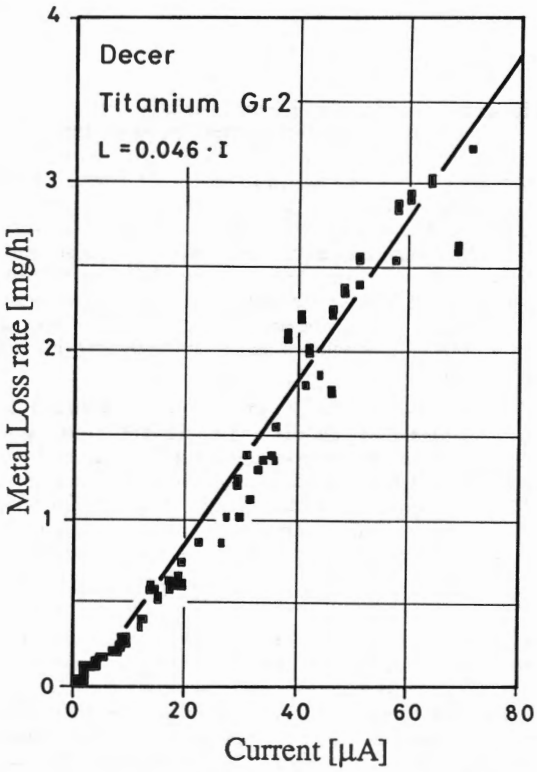


Fig. 1 Vibratory calibration of electrochemical probes.

In most cases cavitation erosion of metallic materials occur by the detachment of small micron size metallic particles from the exposed surface fissured by the repeated impacts of cavitation implosion. For passive metals in aqueous solution this surface cracking and particle detachment generate an electrochemical current directly proportional to the erosion rate [13]. The cavitation erosion detector "DECER" has been developed with titanium probes. Titanium grade 2 has been found the best probe material : it is a well known and characterized metal, readily available, presents a medium cavitation resistance and a strong and reproducible cavitation current signal in most industrial waters. Since the surface passive film is regenerated almost instantaneously the probes are self-regenerating and can give fast response over long periods of time. The best sensitivity and stability is obtained on probes pre-eroded or preincubated by ultrasonic cavitation [9]. As shown on Figure 1, preincubated titanium probes show an average calibration factor in ultrasonic cavitation of 0.05 mg/h per μA or 1.0 mm/a per μA/mm$^2$ with a detection limit of the order of 1μg/h.

Although this calibration factor may increase slightly with cavitation intensity and the average eroded particle size, it was found to be valid for a wide range of cavitation intensity and temperature, between 4 and 40°C, in tap and sea water. This technique is very sensitive: tests in ultrasonic cavitation show that it can detect cavitation intensity that could erode the softest metals. It gives an instantaneous and localized measurement of the erosion rate and the cavitation intensity. It has been used successfully in a variety of laboratory and industrial equipment [14].

## EXPERIMENTAL SET-UP

The IMHEF high-speed cavitation tunnel is specially designed for the study of cavitation in a velocity range of technical interest [15]. A velocity of 50 m/s can be reached in the rectangular test section of 150 mm x 150 mm x 750 mm. The test section itself is equipped with optical windows for visualization. A revolving bed plate flange provides a rigid mounting base for the profile with the capability of varying the angle of incidence.

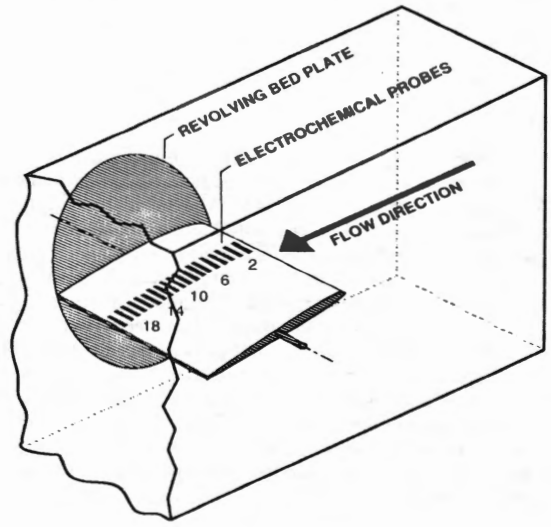


Fig. 2 The instrumented NACA profile.

The blade studied has a symmetrical NACA 009 profile with a maximum thickness of 10 mm. It is truncated at 90% of the chord, the resulting chord length L being 100 mm. As illustrated on Figure 2, 19 isolated titanium probes of 3 mm width and 15 mm length with spot-welded titanium leading wires have been transversely placed every 5 mm all along the chord, the sensitive area of each probes being 43 mm$^2$. A reference titanium probe is flush-mounted on the wall of the test section in a cavitation free area. In order to fulfill the geometry requirement the probes were machined mounted on the profile itself with a N.C. grinding machine, and afterwards pre-eroded by acoustic cavitation. A computer controls data acquisition through the multi-channel potentiostat connected to the 19 probes and the reference probe.

To visualize the cavitation development over profile suction side, high-speed photographs are taken simultaneously with a record of all the flow parameters. The wall pressure distribution of the blade has also been measured by a water pressure line scanning system connected to 19 pressure taps of 0.5 mm diameter and streamwise distributed on the blade every 5 mm.

## EXPERIMENTAL RESULTS

The test conditions are the following:
Upstream velocity: 0 - 44 m/s
Incidence: 0 - 5 degrees
Zero to fully developed cavitation.

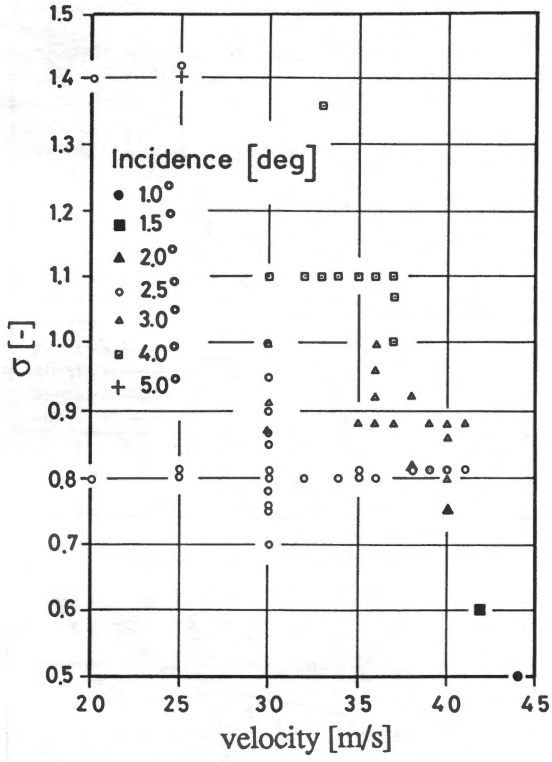


Fig. 3 Set of test operating points.

No measurable erosion has been detected for an upstream velocity of less than 30 m/s and incidence angle of less than 3°, even for conditions with fully developed, collapsing and mildly noisy cavitation. We have therefore concentrated our study to higher velocities and incidence conditions, as shown on Figure 3.

We have gathered on Figure 4 the cavitation erosion rates as obtained through the current given by the electrochemical probes and the calibration curve of Figure 1 for different operating conditions. The erosion rate with respect to the relative streamwise position X/L on the profile is reported in Figures 4-a and 4-b for a velocity range of 30 m/s to 41 m/s and by setting the cavitation number σ and the incidence angle at 0.88, 3° and 1.1, 4° respectively. The cavitation number σ is related to the upstream velocity V and the upstream static pressure p as follows:

$$\sigma = \frac{p - p_v}{\frac{1}{2}\rho V^2}$$

Where $p_v$ is vapor pressure and ρ water density.

We have reported on Figure 4-c the influence of σ on the erosion rate for an upstream velocity V of 36 m/s and an incidence angle of 3°. Figure 4-d shows the influence of the incidence angle for a given velocity and σ value. It should be noticed on these curves that some probes have been short-circuited with the profile during the measurements because of the extreme conditions. This leads to the low signals observed on Figure 4-b at X/L = 0.85; on Figure 4-c at X/L = 0.3; and on Figure 4-d at X/L = 0.55.

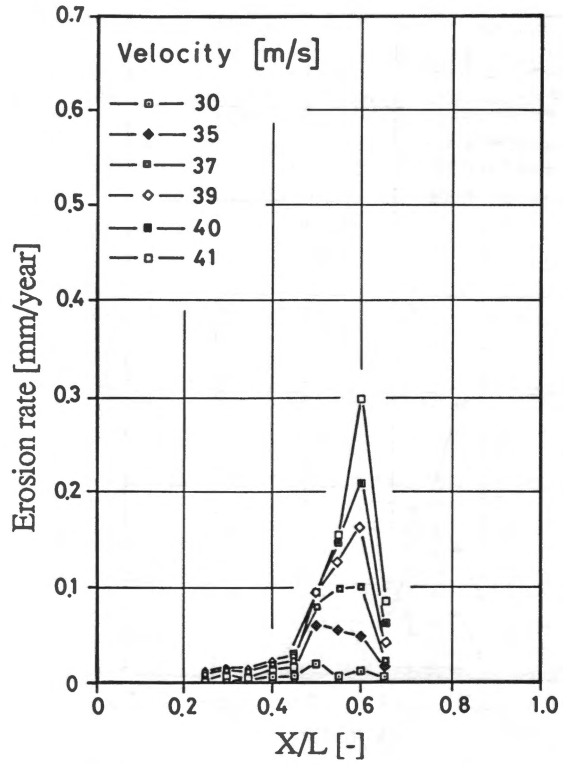


Fig. 4-a Electrochemical DECER erosion results
Incidence = 3 °, σ = 0.88

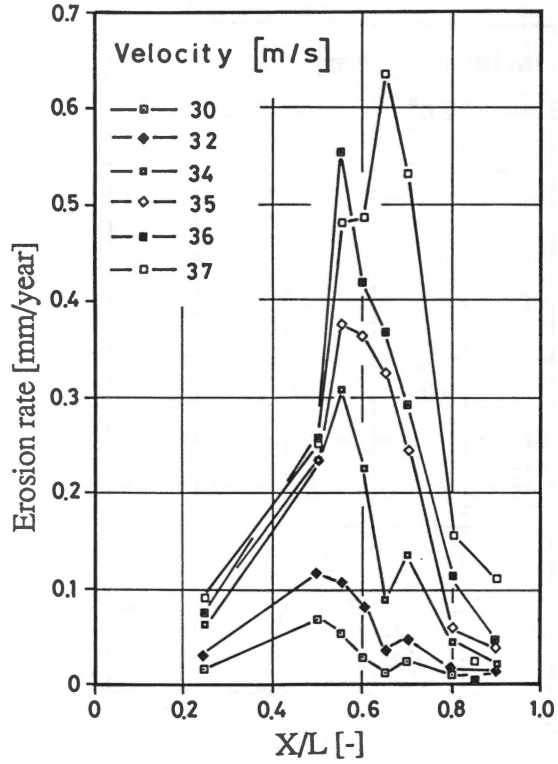


Fig. 4-b Electrochemical DECER erosion results
Incidence = 4 °, σ = 1.1

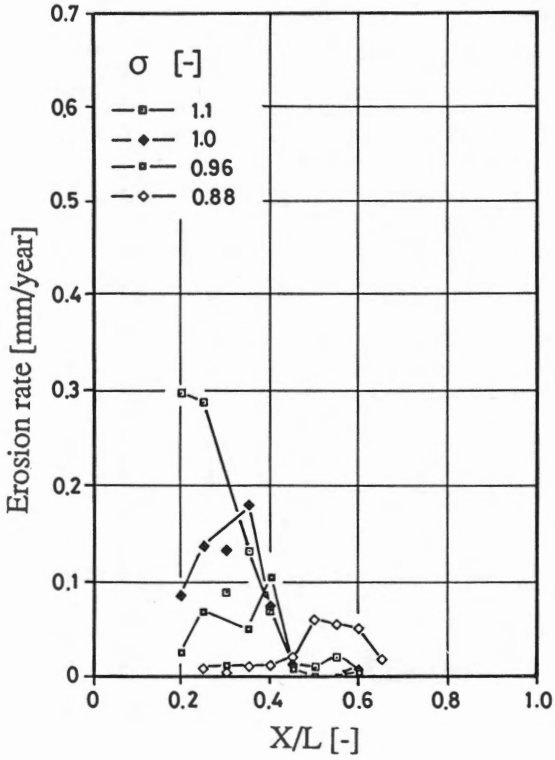


Fig. 4-c Electrochemical DECER erosion results
V = 36 m/s, incidence = 3 °

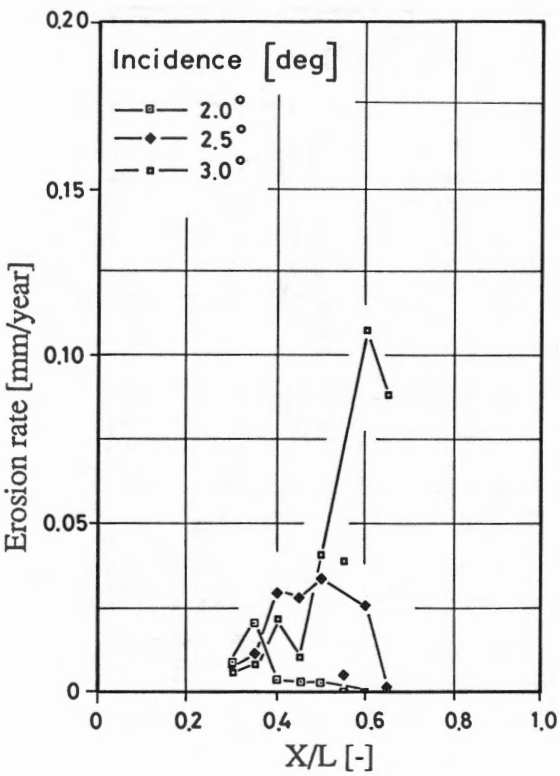


Fig. 4-d Electrochemical DECER erosion results
V= 40 m/s, σ = 0.80

Curves of the wall pressure coefficient $C_p$ on the suction side are given in Figure 5-a through c for the same conditions as Figure 4. In addition we have reported on these curves the location of the maximum erosion rate given by the probes for each condition. These are represented by the shaded rectangles pointing on the corresponding curves.

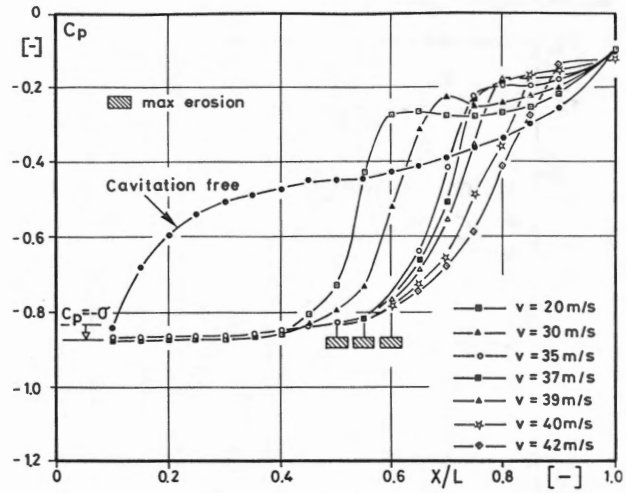


Fig. 5-a Incidence = 3 °, σ = 0.88

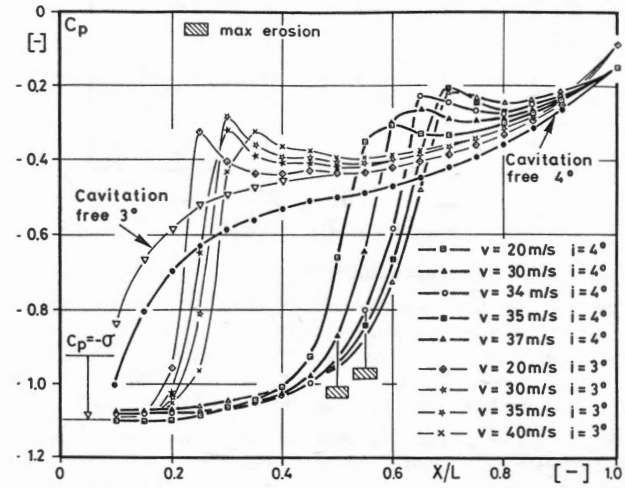


Fig. 5-b Incidence = 3° and 4 °, σ = 1.1

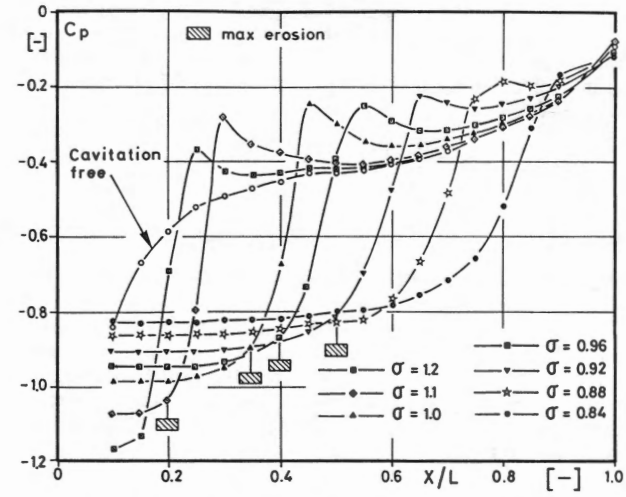


Fig. 5-c V = 36 m/s, Incidence = 3 °

Fig. 5 Distribution of the suction side pressure coefficient

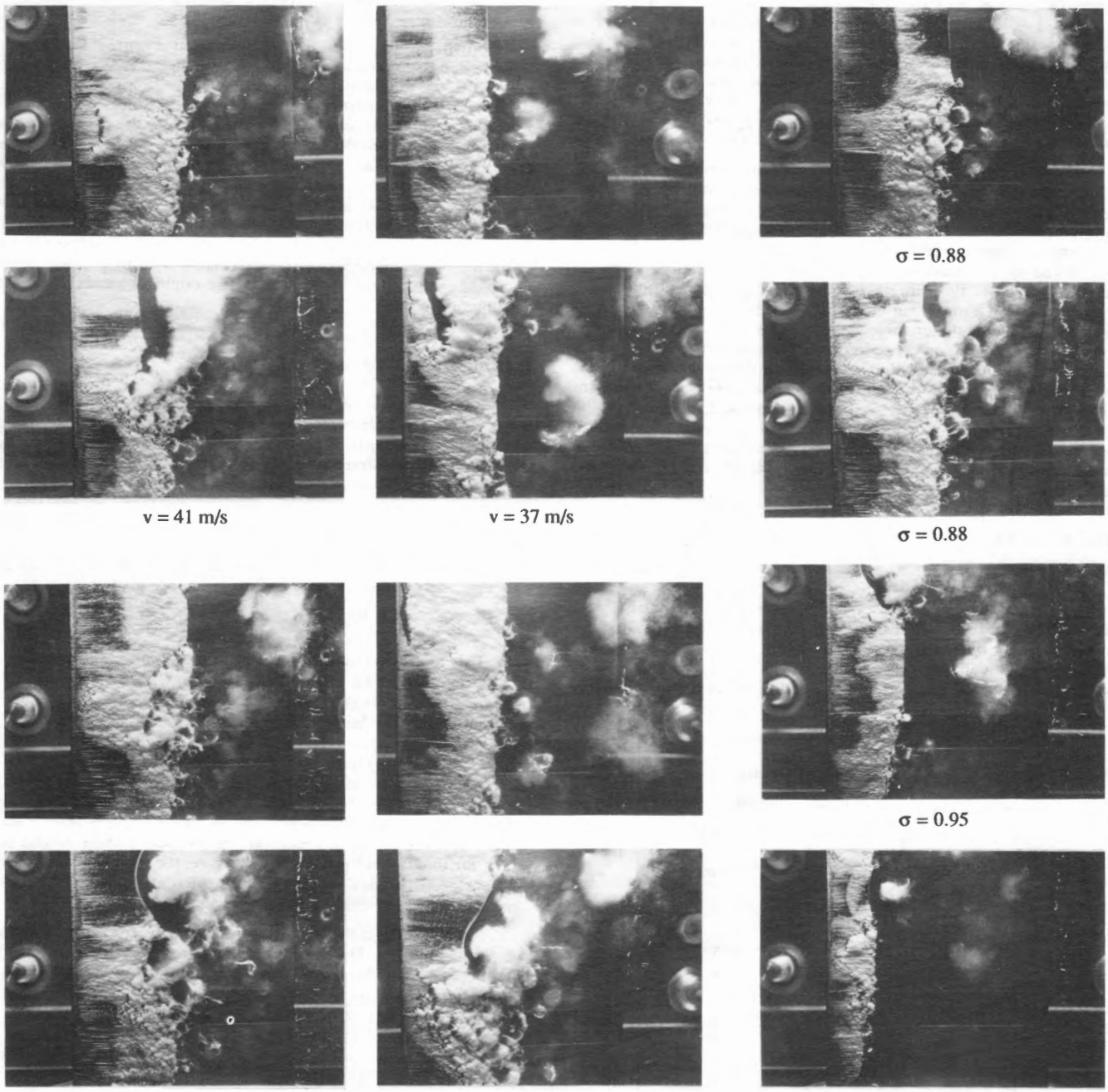


**a) incidence = 3 deg**
**σ = 0.88**

**b) incidence = 4 deg**
**σ = 1.1**

**c) incidence = 3 deg**
**V = 36 m/s**

Fig. 6 Upper views of the cavity development (Flow from left to right)

The photographs shown on Figure 6 have also been taken at the same conditions as the ones on Figure 4. In Figures 6-a and 6-b we present two sets of photographs taken at the two extreme velocities, 30 m/s and 40.7 m/s, for the same $\sigma$ and incidence conditions. For both velocities we have seen two superposed situations: a regular foamy attached leading edge cavity with numerous swirling cavitation structures in its closure region, and the onset of a strong instability of the main cavity leading to the detachment of a part of the cavity itself. Photographs of Figure 6-c show the leading edge cavity development with respect to $\sigma$ by keeping both velocity and incidence constant.

The thin sheet cavitation, quite stable and quiet, observed for inclination angles lower than 3°, always yields very little erosion, even for the highest speeds. Measurable erosion was detected only when the main cavity becomes thicker, unstable and noisier. For the same $\sigma$ value and incidence, Figure 4-a and 4-b, the maximum erosion rate increases as the upstream velocity is increased; its location is slightly displaced towards the outlet edge as the cavitation cloud has a tendency to stretch out when the velocity is increased. For the same velocity, Figure 4-c the erosion rate increases when $\sigma$ is raised from the generalized cavitation conditions. The maximum rate value creeps up and is pushed towards the inlet edge until it finally becomes zero as cavitation is vanishing for higher $\sigma$ values. The same type of behavior is observed when the incidence angle is increased, Figure 4-d; the erosion rate grows with the enlarging and thickening cavitation pocket. It is as well displaced towards the outlet edge since the maximum erosion rate is always located at the closure region of the main cavity.

## DISCUSSION

### The erosive cavities

The comparison between erosion rate distribution and visualization confirms what has been previously noticed [10]: the erosive cavities corresponds to the travelling cavitation swirling structures which collapse in the pressure recovery region of the flow just downstream the closure of the leading edge cavity. This is

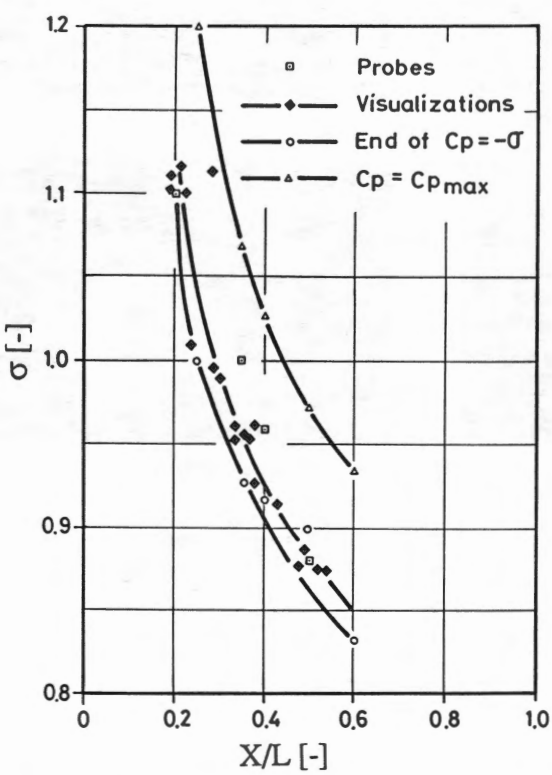


Fig. 7 Maximum erosion rate and cavity closure position V=36 m/s, incidence=3 °

obvious in the following Figure 7 which presents correlation between the location corresponding to the maximum erosion given by the DECER probes and the cavity closure region obtained by visualizations.

Furthermore, when we compare on Figures 5 and 7 the maximum erosion rate location and the pressure coefficient curves, we can observe that erosion occurs within the region of strong instabilities, where part of the main cavity is being shed away. This region of instabilities on Figure 5 corresponds to the region where the Cp curve varies from the $Cp = -\sigma$ step value to a maximum pressure recovery value Cpmax. The maximum erosion occurs at the beginning of the instability area, very close to the region where the pressure coefficient still has a constant $-\sigma$ value, and therefore when the pocket is shrunk to it's extreme as it can be also seen on the photographs of Figure 6. Moreover visualizations indicate that the collapses of parts of the main leading edge cavity, convected out far by the flow, are not responsible for the erosion, even if it could cause high pressure fluctuations levels.

### Erosion threshold

The fact that even well developed leading edge cavity does not produce any appreciable erosion for incidence below 3° and up to 41 m/s seems to confirm the existence of a threshold in the collapse pressure for the erosion of a given material. Since the collapse pressure value can be related to the absolute back pressure level in the pressure recovery region downstream the cavity, we can conclude that this level is not high enough to erode titanium in the case of leading edge cavities corresponding to incidence angle of less than 3°. Thus if $C_{pmax}$ is the maximum of pressure coefficient downstream of the cavity a transient swirling cavity experiences a pressure difference given by :

$$p_{max} - p_v = (C_{pmax} + \sigma)\,\tfrac{1}{2}\rho V^2$$

This relation shows that the pressure collapse and therefore the erosion rate can be increased either through $C_{pmax}$ by increasing the incidence, or by increasing $\sigma$. The role of the upstream velocity will be examined later. The back pressure level influence is well established by the effect of the $\sigma$ value as it is shown on Figures 4-c and 5-c where we see an obvious increase of the term $C_{pmax}+\sigma$ with an increase of the $\sigma$ value. As far as a leading edge cavity can exist the maximum of erosion is increased with the cavitation number. These results confirm the previous observations made by other people and in particular with the same technique on Francis turbine model tests [8, 9]: the maximum localized erosion rate, the most damageable that can perforate blades, occur for intermediate $\sigma$ values between cavitation inception and generalized cavitation.

A small difference in the angle of attack yields great changes of the erosive power. The different Cp curves for the same $\sigma$ and V conditions at 3 and 4 degrees of angle of attack show a greater $C_{pmax}$ value behind the main cavity at 4 degrees. However the increase of this value does not seem to be high enough to totally explain the tremendous change of the erosive power. This change could be explained through an increase of the transient cavity size due to stronger instabilities of the main cavity.

The strong dependance of cavitation erosion with respect to the flow incidence angle and $\sigma$ measured on the NACA profile provides a good explanation for the dramatic increase of erosion on Francis turbines during high load operation, when load is increased from the best efficiency peak to a maximum output. The effect of incidence angle of the NACA profile can then be related to the incidence angle defect of the turbine blades.

### Velocity influence

We can observe two effects of the upstream velocity on the streamwise distribution of the erosion.The first and more obvious effect concerns the tremendous growth of the erosion with respect to the velocity increase. In order to point out the influence of the upstream velocity on the total erosion rate on the profile, we have

integrated the erosion depth rate distributions along the chord for the measurements corresponding to Figure 4-a and 4-b. The results give the mean penetration depth rate expressed in mm per unit time with respect to the velocity as presented on Figure 8. We can see that the erosion rate is proportional to the velocity at the nth power, other conditions being kept constant.

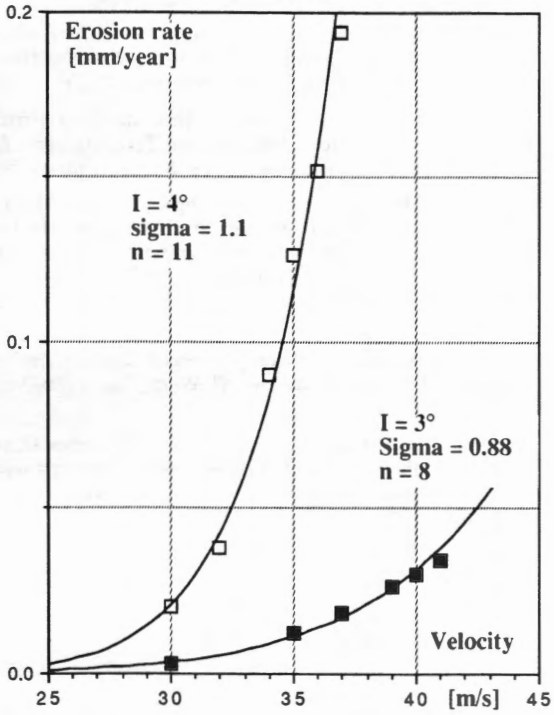


Fig. 8 Mean penetration depth rate integrated over the whole chord length

The second effect of the upstream velocity increase is a downstream displacement of the cavity closure region and therefore a shift of the location where the maximum erosion rate takes place. Both these displacements can be seen on curves of Figures 4a, 4b and Figures 5-a , 5b.

Both this erosion rate growth and spatial shift can be easily explained if we relate this erosion to the collapse of travelling swirling cavities. Visualizations and Laser Doppler Anemometry experiments [10] show that transient cavities, observed in the wake of the leading edge cavity closure, originate from discrete flow structures shed from the beginning of the main cavity with a frequency scaled by the shearing of the flow in this closure region. In this region, the vorticity increase, caused by the stretching of the discrete structure vorticity lines, leads to the formation of inverse U-shaped transient cavities. The cavitation vortices are then advected downstream and the vortex cavity collapses occur close to the blade wall, generating very high pressure shock waves whose intensity can be higher than 1000 MPa [16-17], and producing severe damage to the material. Thus, the swirling structure dynamics leads to a generation rate of erosive cavities with a mean frequency f and a mean vorticity $\omega$ given by:

$$S = \frac{f\,\delta}{U_{ext}} \qquad \text{and } \omega = \frac{U_{ext}}{\delta}$$

where S is a Strouhal number and $\delta$ is a displacement thickness of the shear layer at the cavity closure corresponding to an outer velocity $U_{ext}$.

These parameters allow us to scale up the mean erosive power of the swirling cavities, since this erosive power can be considered as the product of the potential energy of each cavity by their shedding frequency f, the potential energy being evaluated as the product of the pressure difference $p_{max} - p_v$ by the cavity volume. We can see that, if up to now, shedding frequency and back pressure can be measured and computed as well, we need more experiments in order to scale the volume of the swirling cavities as related to the above parameters. Nevertheless a characteristic volume can be build up by making the crude assumption that it can be expressed as one of a cylindrical cavity of diameter d and length l. If we assume a Rankine vortex motion with a solid body rotation core radius of magnitude $\delta$, the cavity diameter d corresponding to the vapor pressure is expressed as follow:

$$\frac{d}{\delta} = 2\sqrt{2 - (C_{pmax} + \sigma)\frac{V^2}{U_{ext}^2}}$$

Cavity length l could be given by any transverse instability wave length analysis. However, we see, obviously, that the lack of experimental data concerning the size of the transient cavities prevents us to provide further informations in order to predict cavitation erosion.

## CONCLUSION

The DECER electrochemical detection technique can be used to quantify and locate cavitation erosion.

Inlet edge sheet cavitation, thin, normally stable and quiet at lower flow incidence angles of the NACA profile, is very little erosive. The erosive power grows rapidly with the incidence of the profile and the water velocity. This growth goes along with noisier and greater unstationary vorticity structures, and a thickening of the main inlet edge cavity. The maximum erosion rate is always localized in the closure region of this main cavity where U-shaped swirling structures strike repeatedly the surface.

These cavitation erosion mechanisms explain the intense localized erosion observed on large Francis runners operated at full load with blade incidence angle defect.

Model tests conducted at lower Reynolds number tests can completely miss that type of cavitation erosion mechanism. Viscous flow calculations is required together with experimental quantitative measures at high Reynolds number such as those provided by the electrochemical technique.

In order to provide a practical cavitation monitoring system acoustic detection will be calibrated with the DECER technique. These measurements should also give more insight into the erosion mechanism by providing the time and frequency spectra.

## ACKNOWLEDGEMENT


The authors wish to acknowledge all their colleagues from the EPFL Cavitation Group and the Hydro-Québec Materials Technology Group. This research is financially supported by Swiss Federal "Commission d'Encouragement à la Recherche Scientifique", Swiss Energy producers association "Nationaler Energie Forschung Fonds", Hydro-Québec, Sulzer Brothers Company and Vevey Engineering Works company.


## REFERENCES


[1] Simoneau, R., "The optimum protection of hydraulic turbines against cavitation erosion", *Proc. 12th IAHR Symposium*, September 1984, Stirling (UK) .

[2] Arndt, R.E.A., Ferreira, A., Rodrigue, P.R.,Sinclair, J.P.,Voigt R.L,"Assessement and Mitigation of Cavitation Pitting in Hydraulic Turbines", *Proc.13th IAHR Symposium*, September 1986 Montréal (Canada)

[3] Simoneau, R.,Mossoba, Y., "Field Experience with Ultra-High Resistance Alloys in Francis Turbines", *Proc. 14th IARH. Symposium*, 20-23 June, 1988, Trondheim (Norway)

[4] Favre, J.N. and Walther, W., "Analyse de la cavitation d'entrée d'un aubage Kaplan par l'application d'une méthode de calcul inverse bi-dimensionnelle", *Proc.13th IAHR Symposium*, September 1986 Montréal (Canada) vol. 1, pp 4.1-4.14 .

[5] Favre, J.N. , Avellan, F. and Ryhming, I.L., "Cavitation Performance Improvement by using a 2-D Inverse Method of Hydraulic Runner Design", *Proceedings of Int. Conf. on Inverse Design Concepts and Optimization in Engineering Sciences-II (ICIDES), 26-28 October, 1987, Pennsylvania State University (USA)*, pp.15-1, 15-15

[6] Lecoffre, M., Grison, P., Michel, J.M., "Prévision de l'Érosion de Cavitation pour les Turbomachines", *Proc.13th IAHR Symposium,* September 1986 Montréal (Canada)

[7] Karimi, A., Maamouri, M., "New approach for cavitation erosion rate computation", *Proceedings of 7th Int. Conf. on Erosion by Liquid and Solid Impact,* 6-10 September 1987, Cambridge (UK), pp 27-1, 27-8.

[8] Bourdon, P., Simoneau, R., Désy, N., Do, N., Grenier, R., "Solving a Severe Cavitation Erosion Problem on a 50 MW Francis Turbine.", *Proc. 14th IARH. Symposium,* 20-23 June, 1988, Trondheim (Norway)

[9] Simoneau, R., Bourdon, P., Désy, N., Grenier, R., "Cavitation Detection in Model Tests of Hydraulic Turbines" *Canadian Electrical Association Report #230G439,* Jan. 1988.

[10] Avellan, F., Dupont, Ph., "Cavitation Erosion of Hydraulic Machines: Generation and Dynamics of Erosive Cavities." *Proc. 14th IARH Symposium* , 20-23 June, 1988, Trondheim (Norway).

[11] Avellan, F., Dupont, Ph., Ryhming, I.L., "Generation mechanism and dynamics of cavitation vortices downstream of a fixed leading edge cavity", *Proc. of 17th Symposium on Naval Hydrodynamics*, The Hague (The Netherlands), August 29- September 2, 1988, Sessions V, pp 1 13.

[12] Einsenberg, P., Preiser, H.S., Thiruvengadam, A.T., "On the Mechanism of Cavitation Damage and Methods of Protection" *Trans. Society of Naval Architects*, Dec 1966.

[13] Simoneau, R., Fihey, J.L., Chincholle, L.,"Effet d'Activation Anodique de la Cavitation Érosive", *Proc. 11th IARH Symposium* , September 1982, Amsterdam (NL)

[14] Chincholle, L.H., "Study of the Instantaneous Erosion of Cavitation, versus Flow, Pressure and Temperature", *Journal of Hydraulic Research*, Vol. 26, 1988, No. 1, pp. 67-82.

[15] Avellan, F., Henry, P., and Ryhming I., "A New High-Speed Tunnel for Cavitation Studies in Hydraulic Machinery", *Proceedings of International Symposium on Cavitation Research Facilities and Techniques,* ASME Winter Annual Meeting, Boston (USA), December, 1987, FED: Vol. 57, pp. 49-60.

[16] Karimi, A.,Avellan, F., "Comparison of Erosion Mechanisms in Different Types of Cavitation", *Wear,* Dec.1986, Vol. 113, No. 3, pp 305-322.

[17] Avellan, F., and Karimi, A., "Dynamics of Vortex Cavitation involved in the Erosion of Hydraulic Machines", *Proceedings of 7th Int. Conf. on Erosion by Liquid and Solid Impact,* 610 September 1987, Cambridge (UK),.pp 25-1, 25-8.